Paracatenula, an ancient symbiosis between thiotrophic *Alphaproteobacteria* and catenulid flatworms

Harald Ronald Gruber-Vodicka[a,1], Ulrich Dirks[a], Nikolaus Leisch[a], Christian Baranyi[b,2], Kilian Stoecker[b,3], Silvia Bulgheresi[c], Niels Robert Heindl[a,c], Matthias Horn[b], Christian Lott[d,e], Alexander Loy[b], Michael Wagner[b], and Jörg Ott[a]

Departments of [a]Marine Biology, [b]Microbial Ecology, and [c]Genetics in Ecology, University of Vienna, A-1090 Vienna, Austria; [d]Symbiosis Group, Max Planck Institute for Marine Microbiology, D-28359 Bremen, Germany; and [e]Elba Field Station, Hydra Institute for Marine Sciences, I-57034 Campo nell'Elba, Italy

Edited by Nancy A. Moran, Yale University, West Haven, CT, and approved May 31, 2011 (received for review April 8, 2011)

Harnessing chemosynthetic symbionts is a recurring evolutionary strategy. Eukaryotes from six phyla as well as one archaeon have acquired chemoautotrophic sulfur-oxidizing bacteria. In contrast to this broad host diversity, known bacterial partners apparently belong to two classes of bacteria—the *Gamma-* and *Epsilonproteobacteria*. Here, we characterize the intracellular endosymbionts of the mouthless catenulid flatworm genus *Paracatenula* as chemoautotrophic sulfur-oxidizing *Alphaproteobacteria*. The symbionts of *Paracatenula galateia* are provisionally classified as "*Candidatus* Riegeria galateiae" based on 16S ribosomal RNA sequencing confirmed by fluorescence in situ hybridization together with functional gene and sulfur metabolite evidence. 16S rRNA gene phylogenetic analysis shows that all 16 *Paracatenula* species examined harbor host species-specific intracellular *Candidatus* Riegeria bacteria that form a monophyletic group within the order *Rhodospirillales*. Comparing host and symbiont phylogenies reveals strict cocladogenesis and points to vertical transmission of the symbionts. Between 33% and 50% of the body volume of the various worm species is composed of bacterial symbionts, by far the highest proportion among all known endosymbiotic associations between bacteria and metazoans. This symbiosis, which likely originated more than 500 Mya during the early evolution of flatworms, is the oldest known animal–chemoautotrophic bacteria association. The distant phylogenetic position of the symbionts compared with other mutualistic or parasitic *Alphaproteobacteria* promises to illuminate the common genetic predispositions that have allowed several members of this class to successfully colonize eukaryote cells.

intracellular symbiosis | marine catenulid | meiofauna | subtidal sand

Marine catenulid flatworms of the genus *Paracatenula* have no mouth or gut (1). Instead, they harbor intracellular microbial endosymbionts in bacteriocytes (2) that form a tissue known as the trophosome (Fig. 1*A*) in functional analogy to the trophosome of the mouthless Siboglinidae (Annelida) (3). The trophosome almost completely fills the posterior part of the body behind the brain (2, 3). The worms inhabit the interstitial space of warm temperate to tropical subtidal sands together with other animals such as nematodes, gutless oligochaetes, and lucinid or solemyid bivalves that all harbor chemoautotrophic sulfur-oxidizing bacteria (SOB). By migrating through the redox potential gradient in the uppermost 5- to 15-cm sediment layer, millimeter-sized worms can supply chemoautotrophic symbiotic bacteria alternately with spatially separated electron donors and acceptors such as sulfide and oxygen, as has been described for Nematoda and Oligochaeta (4, 5).

Chemosynthetic carbon fixation by using reduced sulfur compounds (i.e., thiotrophy) is widespread in free-living members of the microbial domains *Bacteria* and *Archaea*. This metabolic capability has been found in members of the *Actinobacteria*, *Aquificae*, *Bacilli*, *Chloroflexi*, *Chlorobi*, and *Spirochaeta*, and all classes of the *Proteobacteria* and the archaeal order *Sulfolobales*. One archaeon, "*Candidatus* Giganthauma karukerense" (6), as well as a wide range of protists and animals, including Ciliata (e.g., *Zoothamnium*), Nematoda (Stilbonematinae and *Astomonema*), Arthropoda (*Rimicaris* and *Kiwa*), Annelida (e.g., *Riftia* or *Olavius*), along with bivalve and gastropod Mollusca (e.g., *Solemya* or *Neomphalina*; reviewed in ref. 7), have established themselves as hosts in symbioses with SOB. They all derive some or all of their energy demands from the primary production of the symbionts (7). Interestingly, despite this great taxonomic variety of hosts—from habitats as divergent as deep-sea hydrothermal hot vents, cold seeps, whale or wood falls, and peat and shallow-water sediments—the SOB symbiont diversity seemed to be limited to *Proteobacteria* of the *Gamma* and *Epsilon* classes (7). Here, we present evidence that the symbionts of *Paracatenula* form an ancient clade of sulfur-oxidizing *Alphaproteobacteria* that are strictly coevolved with their hosts and that equal host biomass in the consortium.

Results and Discussion

The body plan of *Paracatenula* suggests that the symbionts make up a substantial proportion of the worms. To specify symbiont-to-host tissue ratios, cross-sections in the trophosome region of three species of *Paracatenula* were analyzed by transmission EM (TEM). The symbionts make up 36.7% of the cross section area in *Paracatenula galateia* (3) (Carrie Bow Cay, Belize), 41.2% in *P.* cf. *galateia* (Dahab, Egypt), and 51.9% in *P.* cf. *polyhymnia* (Dahab, Egypt; Fig. S1). The symbiont-housing trophosome region accounts for 90% to 98% of the total worm length: multiplying these two factors, we roughly estimate symbiont-to-host tissue ratios of 33% in *P. galateia*, 40% in *P.* cf. *galateia*, and 50% in *P.* cf. *polyhymnia*. These are the highest proportions of all known endosymbioses between bacteria and metazoans, far higher

Author contributions: H.R.G.-V., S.B., N.R.H., M.H., A.L., M.W., and J.O. designed research; H.R.G.-V., U.D., N.L., C.B., K.S., C.L., and J.O. performed research; M.W. contributed new reagents/analytic tools; H.R.G.-V., U.D., N.L., C.B., K.S., and J.O. analyzed data; and H.R.G.-V. wrote the paper.

The authors declare no conflict of interest.

This article is a PNAS Direct Submission.

Freely available online through the PNAS open access option.

Data deposition: The sequences reported in this paper have been deposited in the GenBank database [accession nos. HQ689139 (*aprA*); HQ840958 (*cbbM*); HQ689138 (*dsrAB*); HQ689029–HQ689053, HQ689087–HQ689095, HQ689123, HQ689124, HQ689128, HQ689129, and HQ845108–HQ845110 (16S rRNA); HQ689054–HQ689068, HQ689096–HQ689108, HQ689125, and HQ689130–HQ689133 (18S rRNA); and HQ689069–HQ689086, HQ689109–HQ689122, HQ689126, HQ689127, and HQ689134–HQ689137 (28S rRNA)].

[1]To whom correspondence should be addressed. E-mail: harald.gruber@univie.ac.at.

[2]Present address: Department of Marine Biology, University of Vienna, A-1090 Vienna, Austria.

[3]Present address: Project Group Bioresources, Fraunhofer Institute for Molecular Biology and Applied Ecology, D-35394 Giessen, Germany.

This article contains supporting information online at www.pnas.org/lookup/suppl/doi:10.1073/pnas.1105347108/-/DCSupplemental.

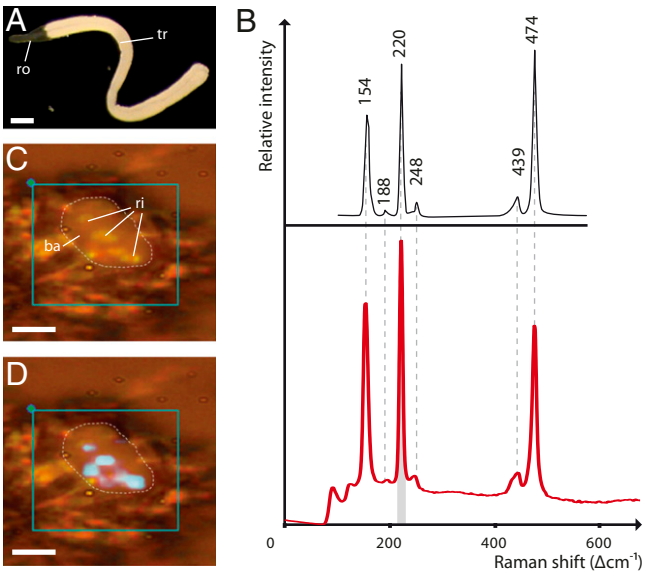

Fig. 1. Sulfur storage in *Candidatus* Riegeria galateiae. (*A*) Living specimen of *P. galateia*, with *Cand*. Riegeria galateiae endosymbionts in trophosome (tr) appearing white in incident light in contrast to the bacteria-free rostrum (ro). (Scale bar: 250 μm.) (*B*) Raman spectrum of individual cellular inclusion (red) with reference spectrum (black) of elemental sulfur in S_8 ring configuration. (*C*) Air-dried *Cand*. Riegeria galateiae cell (ba) with light refracticle inclusions (ri). (Scale bar: 5 μm.) (*D*) Mapping of the Raman sulfur spectrum peak indicated in *B* in gray onto *C*, with the mapped area indicated with turquoise rectangle. (Scale bar: 5 μm.)

than, e.g., in the deep-sea tubeworm *Riftia pachyptila*, in which bacteria make up only 24.1% of the trophosome, which in turn occupies less than one third of the body volume (8). The exceptional proportion of bacterial biomass in this intracellular symbiosis questions the common view that animals exploit the metabolic skills of their microbial partners because the *Paracatenula* worms in return appear to serve as a protective vehicle for their symbionts.

The bacteria of all *Paracatenula* species contain highly light refractive spherical inclusions (0.5–2 μm in diameter), which render the bacteria white in incident light (Fig. 1*A*). This white coloring, typical for SOB that store elemental sulfur (9), was an initial clue that the symbionts could be sulfur oxidizing (2). We selected the symbionts of *P. galateia* for a detailed analysis because the worms are abundant, comparatively large, and morphologically distinct (3). Sulfur oxidizing capabilities were assessed by examining sulfur storage and functional genes used in thiotrophy. All inclusions of extracted symbiont cells from *P. galateia* analyzed by Raman microspectroscopy consist of elemental sulfur in S_8 ring configuration (Fig. 1 *B*–*D*). Energy dispersive X-ray microanalysis shows that in the trophosome this bacterial sulfur storage can make up 5% to 19% of the tissue mass (Fig. S2). In many SOB that store elemental sulfur, the sirohaem dissimilatory sulfite reductase (i.e., DsrAB) enzyme system functioning in reverse is an important part of the sulfur oxidation machinery (10). Our phylogenetic analysis of a collection of dissimilatory sulfite reductase (i.e., DsrB) sequences from SOB, including the sequence of the *P. galateia* symbionts determined in the present study, demonstrates that the sequences of *Paracatenula* symbionts form a well supported monophyletic clade with sequences from other thiotrophic *Alphaproteobacteria* [approximate likelihood-ratio test (aLRT), 0.90; posterior probability (pp), 1.00; Fig. S3]. This corroborates the results from a previous study placing the DsrAB sequences from bacteria associated with two species of *Paracatenula* together with sequences of the alphaproteobacterial genus *Magnetospirillum*, albeit with weak node support (10). Additionally, the gene coding for AprA, the α-subunit of dissimilatory adenosine-5′-phosphosulfate (APS) reductase, another key enzyme in sulfur energy metabolism, was partially sequenced for the *P. galateia* symbionts. APS reductase is used by SOB to oxidize sulfite to APS and by sulfate-reducing microorganisms to reduce APS to sulfite (11). The symbionts' AprA sequence clusters with the AprA lineage II of SOB with good statistical support (aLRT, 0.89; pp, 1.00; Fig. S4). The Calvin–Benson–Basham pathway with ribulose-1,5-bisphosphate carboxylase/oxygenase (RubisCO) as the central enzyme is a key mechanism of carbon fixation in autotrophic organisms (12). The partial sequence coding for RubisCO form II (CbbM) sequenced for the *P. galateia* symbionts is related to sequences from the alphaproteobacterial genus *Magnetospirillum* and other chemoautotrophs (Fig. S5).

Taken together, three lines of evidence point to a chemoautotrophic sulfur-oxidizing lifestyle of the symbionts: (*i*) the habitat that *P. galateia* shares with many other hosts of thiotrophic bacteria, (*ii*) intracellular storage of elemental sulfur by the symbionts, and (*iii*) the presence of *cbbM* as well as *dsrAB* and *aprBA*, both related to sequences from SOB, in the symbionts' genome.

16S rRNA gene based approaches were used to assess the diversity within and between the symbiont populations of individual worms of *Paracatenula galateia*. The PCR products obtained separately from 10 specimens using general bacterial 16S rRNA gene primers comprise the same phylotype based on (*i*) clone libraries, (*ii*) direct sequencing, and (*iii*) denaturing gradient gel electrophoresis (DGGE) analysis [pairwise identity of 99.7–100; a species-level phylotype threshold of ≥99% 16S rRNA gene sequence identity was used (13)]. According to the ribosomal database project classifier (14) and our comprehensive phylogenetic analysis (as detailed later), this bacterial phylotype is a member of the alphaproteobacterial order *Rhodospirillales* (Fig. 2). FISH with a phylogenetically nested probe set specifically targeting most *Bacteria*, most *Alphaproteobacteria*, and the symbiont confirms that *P. galateia* contains only one alphaproteobacterial species-level phylotype (Fig. 3).

To infer host specificity of the symbionts from different *Paracatenula* hosts and to elucidate the symbionts' evolutionary relationships, we sequenced symbiont 16S rRNA genes from additional 31 worms belonging to 15 species, all morphologically distinct from *P. galateia*: five species from the Caribbean Sea (Carrie Bow Cay,

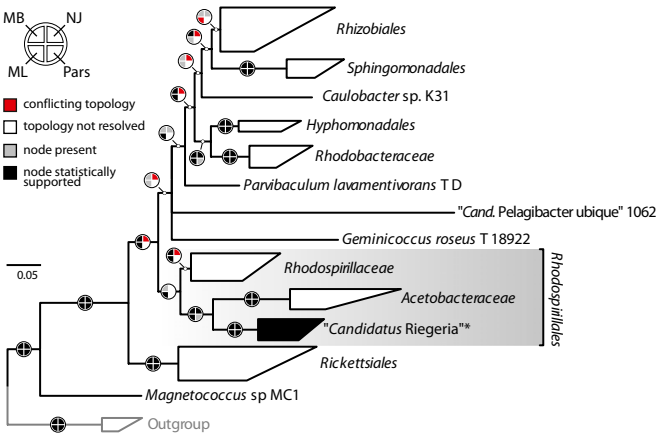

Fig. 2. Phylogeny of the family level *Candidatus* Riegeria clade in the *Alphaproteobacteria*. Based on comparative 16S rRNA gene analysis, the *Cand*. Riegeria clade is the sister group of the family *Acetobacteraceae* within the order *Rhodospirillales*. The tree shown was estimated by using MrBayes (MB), and node support is additionally indicated for three alternative methods (NJ, neighbor joining; Pars, parsimony; ML, maximum likelihood). **Cand*. Riegeria clade; the detailed phylogeny of this clade is shown in Fig. S6. (Scale bar: 5% estimated sequence divergence.)

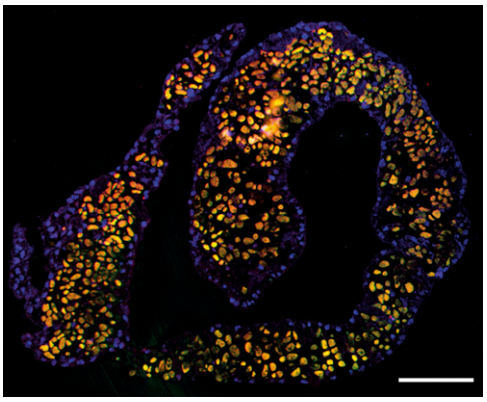

Fig. 3. *Candidatus* Riegeria galateiae in the host trophosome. Laser scanning confocal micrograph of FISH on LR-White cross-section; Overlay of three images with a bacteria-specific probe (green), symbiont-specific probe (red), and eukaryote-specific probe (blue). Because of the overlay of colors, the symbionts appear in yellow. (Scale bar: 50 μm.)

Belize), one from the Mediterranean Sea (Elba, Italy), five from the Red Sea (Dahab, Egypt), and four from the Pacific Ocean (Lizard Island, Australia). Our 16S rRNA gene-based tree of the *Alphaproteobacteria* (Fig. 2) is largely congruent with the topologies presented in recent phylogenomic studies of this class (15, 16). The placement of the symbiont sequences shows that (*i*) the symbionts form a distinct and well supported sister clade to the *Acetobacteraceae* within the order *Rhodospirillales* (Fig. 2), (*ii*) the symbionts are present in all worms (Fig. S6), and (*iii*) each host species harbors only one phylotype, which is specific for the respective host (Fig. S6). Based on these phylogenetic data and our detailed metabolic analysis, we propose the provisional classification (17) "*Candidatus* Riegeria galateiae" for the symbionts of *P. galateia*. Short description is as follows: coccoid alphaproteobacterium of the order *Rhodospirillales*, 5 to 8 μm in diameter with intracellular storage of elemental sulfur, present in bacteriocytes of the catenulid flatworm *Paracatenula galateia*. The basis of assignment is as follows: 16S rRNA gene, *cbbM*, *dsrAB*, and *aprA* sequences (HQ689043, HQ840958, HQ689138, and HQ689139, respectively) and hybridization with the phylotype-specific oligonucleotide probe PAR1151 (5′-CTT GTC ACC GGC AGT TCC CTC-3′). Riegeria refers to the late zoologist Reinhard Rieger, who described the host genus, together with W. Sterrer (1); and galateiae to its specific flatworm host *P. galateia*.

Our phylogenetic analysis also revealed that only a single 16S rRNA sequence in public databases (GQ402753) belongs to the clade of *Paracatenula* symbionts (Fig. S6). This clone was retrieved from a permanently waterlogged tropical peat swamp forest sample in Thailand (18), but only scarce details are available for the sample.

The maximum 16S rRNA gene sequence divergence within the symbiont clade is 12.7%, and members of the clade show a minimum sequence divergence of 11.5% to the next described relative *Elioraea tepidiphila* TU-7 (EF519867). This high degree of phylogenetic distinctness is in the range reported for other proteobacterial families (19) and would thus merit, from a 16S rRNA-based point of view, the proposal of a family within the *Rhodospirillales* to classify the *Paracatenula* symbionts.

With the exception of the genus *Paracatenula*, all groups of Catenulida have a cosmopolitan distribution ranging from tropical to cold temperate; several species of the marine catenulid genus *Retronectes*, which have no chemosynthetic symbionts, have been found as far north as Kristineberg on the Swedish west coast (1, 20). As all cultured *Rhodospirillales* related to the symbionts are mesophilic or slightly thermophilic (21), it is tempting to speculate that the limitation of *Paracatenula* to warm temperate or tropical waters reflects the temperature requirements of its symbionts.

To molecularly characterize the different hosts, we sequenced their 18S and 28S rRNA genes. Our phylogenetic analysis corroborates the placement of *Paracatenula* within the Catenulida as the monophyletic sister clade to the limnic *Catenula*/*Suomina* species complex (20) (Fig. S7). A strict consensus tree based on several phylogenetic methods using all hosts with both 18S and 28S rRNA genes sequenced (15 species) is highly congruent to the 16S rRNA gene tree obtained for their symbionts (Fig. 4). Bayesian inference-based reconstructions for this dataset are fully resolved on the host species level and completely congruent between host and symbiont (Fig. S6). The cocladogenesis of both groups indicates that a common ancestor of the host worms had acquired an alphaproteobacterial progenitor of the *Cand*. Riegeria clade and that this association has been stably maintained up to the present day by vertical transmission of the symbionts from one host generation to the next (22). In chemoautotrophic associations, vertical symbiont transmission has been reported

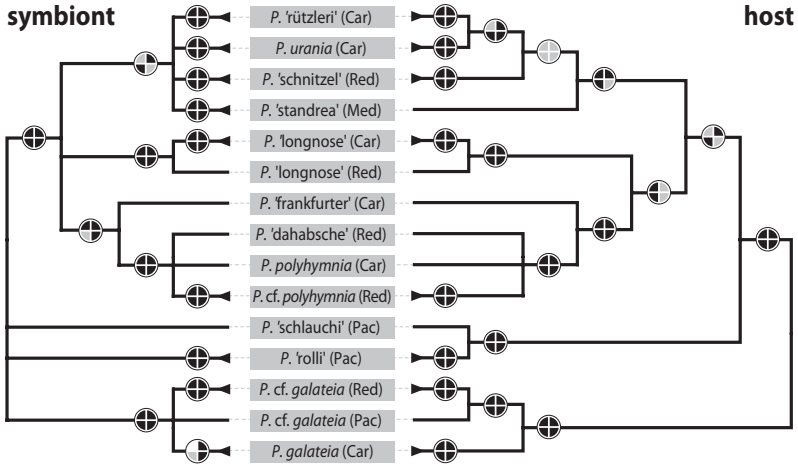

Fig. 4. Cocladogenesis between *Paracatenula* and *Candidatus* Riegeria. Tanglegram of strict consensus cladograms of four reconstruction methods for both symbiont 16S rRNA and host concatenated 18S and 28S rRNA. Node support is indicated as in Fig. 3. Provisional working names for undescribed species are given in parentheses. Sample origins: Car, Caribbean Sea; Med, Mediterranean Sea; Red, Red Sea; Pac, Pacific Ocean. No conflicting nodes are statistically supported in the results of the four phylogenetic reconstruction algorithms, indicating close coevolution between the partners.

only for the deep-sea clam family Vesicomyidae (23). Recent studies, however, have shown that host–symbiont phylogenies are decoupled for some vesicomyid clams, suggesting a mixed mode of symbiont transmission with vertical transmission occasionally interrupted with lateral symbiont acquisition (24, 25). Vertically transmitted symbionts tend to have an accelerated nucleotide substitution rate compared with free-living bacteria (26, 27). Sequence divergence of 16S rRNA for inheritable symbionts averages approximately 4% for every 100 million years (Ma), ranging from 2.5% to 11%, whereas free-living bacteria have rates ranging from 2% to 4% for 100 Ma (26, 28, 29). Based on this range of rates, the symbiosis in the ancestor of *Paracatenula* was established between 100 and 635 Mya. The maximum estimated divergence time for flatworms is 620 Ma and must be used as the maximum age of this symbiosis (30). As the *Cand*. Riegeria symbionts have no detectable nucleotide substitution rate heterogeneity in their 16S rRNA gene sequences compared with free-living *Acetobacteraceae* (Tajima rate test, $P > 0.05$ for all *Cand*. Riegeria against the *Acetobacteraceae* used in the phylogenetic analysis), we suppose a divergence rate of 2.5% in 100 Ma, as has been documented for symbionts with only slightly accelerated rates. This delimits the estimated age to 500 to 620 Ma. In comparison, the ancient solemyid and lucinid bivalve lineages in which all living taxa harbor chemoautotrophic symbionts have a paleontological record dating back to the late Ordovician/early Silurian 445 to 435 Mya (31). Even with the uncertainties involved when using evolutionary rates established for other groups of symbionts (29), the *Cand*. Riegeria–*Paracatenula* association can be considered the oldest known mutualistic bacteria–metazoan symbiosis, likely dating back to the early evolution of bilaterian diversity in the late Ediacaran/early Cambrian.

Coevolving inherited endosymbionts tend to have guanine and cytosine (GC) depleted genomes (27, 32). The alphaproteobacterial families closely related to the *Cand*. Riegeria clade, the *Acetobacteraceae* and *Rhodospirillaceae*, have a very high genomic guanine and cytosine content (gGC; 60–71% and 62–69%, respectively). Although there are no gGC data for *Cand*. Riegeria galateiae yet, the *dsrAB*, *aprA*, and *cbbM* genes combined have a GC content of 51.4%. This significantly lower GC content compared with closely related free-living groups has two possible non mutually exclusive explanations: (*i*) the intracellular symbiosis has relieved the symbionts from the selection pressure that leads to the high gGC in *Rhodospirillales* and the symbiont gGC therefore decreased to approximately 50%; or (*ii*) population bottlenecks leading to high genetic drift (33) have been driving the nucleotide bias in *Cand*. Riegeria galateiae, but at a much slower pace compared with that documented in the less than 50 Ma old symbiosis in vesicomyid clams (symbiont genome sizes of 1.02–1.16 Mb, gGC of 31.6–34%; closely related free-living *Thiomicrospira crunogena* genome size, 2.43 Mb, gGC of 43.1%) (23, 34, 35). The close coevolution of *Paracatenula* and *Cand*. Riegeria, in which each host maintains a monoculture of its specific symbiont, will allow comparative genomic studies to test these hypotheses and other theoretical predictions of genome evolution developed for intracellular symbionts (36). Moreover, this ancient clade of endosymbionts, with their distant phylogenetic position and their different function compared with other symbiotic *Alphaproteobacteria*, could help illuminate the common genetic predispositions that have allowed several members of this class to become successfully incorporated into eukaryotic cells—be it as intracellular parasites such as members of the order *Rickettsiales* or mutualists such as members of the order *Rhizobiales* or of the *Cand*. Riegeria clade.

Methods

TEM. TEM specimens were fixed in glutaraldehyde, postfixed with osmium tetroxide, and, after dehydration, embedded in Low Viscosity Resin (Agar Scientific). Complete ultrathin cross-sections mounted on formvar-coated slot grids were poststained with uranyl acetate and lead citrate. To estimate tissue ratios, digital images of the sections were merged and host and bacterial tissue were digitally traced into vector-based black and white representations. Area calculations were performed with ImageJ software based on these trace images using the "analyze particles" function.

SEM and Energy-Dispersive X-Ray Microanalysis. Specimens were immediately fixed as for TEM analysis. The samples were partly dehydrated in an acetone series up to 75% to preserve a maximum amount of sulfur (37). The samples were embedded in Spurr epoxy resin. Semithin cross sections (2.5 μm) of embedded samples were cut, mounted on carbon-padded stubs, and carbon-coated. The analysis was carried out on a Philips XL20 SEM with an EDAX P-505 sensor using EDAX eDXi V2.11 software. Sulfur was mapped against carbon and at least two other elements prominent in the given spectrum (e.g., phosphorous and osmium) to rule out structural and edge effects.

Raman Microspectroscopy. Extracted symbiont cells of PFA-fixed specimens were mounted on a calcium fluoride slide and analyzed with a LabRAM HR800 confocal Raman microspectroscope (HORIBA Jobin-Yvon). A 532-nm Nd:YAG laser provided the excitation for Raman scattering. Cells were selected haphazardly using a 50× objective, and the signal was acquired over a period of 5 s using a D0.6 intensity filter. The pinhole of the Peltier-cooled CCD detector was adjusted to 250 μm (optical slice, 4.6 μm). Spectra were measured between 0 and 2,000 cm^{-1}. They were baseline-corrected and normalized with LabSpec software 5.25.15 (HORIBA Jobin-Yvon). Reference spectra for elemental sulfur in S_8 ring configuration (Merck) were obtained by using the same settings and methods.

DNA Extraction, PCR Amplification, and Sequencing. DNA was extracted from individual worms by using the Blood and Tissue DNA extraction kit (Qiagen), and 2 μL of each extraction were used as PCR templates. Symbiont 16S rRNA-gene fragments (approximately 1,500 nt) were amplified with bacterial primers 616V (5′-AGAGTTTGATYMTGGCTC-3′) (38) and 1492R 5′-GGYTACCTTGTTACGACTT-3′ (39). PCR products were purified by using the MinElute PCR purification kit (Qiagen) and either directly sequenced with the PCR primers or cloned by using pCR2.1-TOPO and the TOPO TA Cloning Kit (Invitrogen Life Technologies). Host 18S and 28S rRNA-gene fragments (approximately 1,750 and 1,350 nt long, respectively) were amplified for each worm with general eukaryote primers 1f (5′-CTGGTTGATYCTGCCAGT-3′) and 2023r (5′-GGTTCACCTACGGAAACC-3) for 18S (40) and the primers D1a (5′-CCCSCGTAAYTTAAGCATAT-3′) and D5b2 (5′-CGCCAGTTCTGCTTACC-3) for 28S (41). PCR products were purified as described earlier and directly sequenced with the PCR primers. From *P. galateia* samples, *aprBA* was amplified with primers AprB-1-FW (5′-TGCGTGTAYATHTGYCC-3′) (11) and AprA-9-RV (5′-CKGWAGTAGTARCCSGGSYA-3′) (42), *dsrAB* was amplified with primers rDSR1Fa (5′-AARGGNTAYTGGAARG-3′) and rDSR4Rb (5′-GGRWARCAIGCNCCRCA-3′) (10), and *cbbM* was amplified with shortened primers after Blazejak et al. (43): CbbMF_bl_s (5′-ATCATCAARCCSAARCTSGGYC-3′) and CbbM1R_bl_s (5′-SGCRCCRTGRCCRGCMC-3′). We used touchdown PCR cycling programs for *cbbM*, *aprBA* and *dsrAB* as described for *aprBA* in Meyer and Kuever (42). The 395 nt-long *cbbM* fragment was directly sequenced by using the PCR primers, whereas the *aprBA* (2,178 nt) and *dsrAB* (1,911 nt) PCR products were gel purified using the MinElute gel extraction kit (Qiagen) and cloned as described earlier. For all cloned products, at least four clones were randomly picked and fully sequenced with the vector-specific primers M13F and M13R; for *aprBA* and *dsrAB*, we additionally used internal sequencing primers AprA-1-FW and AprB-5-RV (42) and DSR874F (10).

DGGE Analysis. DGGE analysis of 16S rRNA genes was performed as described by Meyer et al. (44). In every lane, only one band was observed, which was excised from the DGGE gel, and gel slices were stored in 50 mL MQ overnight at 4 °C. One microliter of this elution was used as a template for PCR reamplification using the forward primer (341f) without the GC clamp. Reamplifed DNA was purified and directly sequenced as described above.

rRNA Gene Based Phylogenetic Analyses. A 16S rRNA gene dataset for *Alphaproteobacteria* was constructed including 41 *Cand*. Riegeria sequences, three BLAST (45) hits from GenBank longer than 1,400 bp with sequence identities more than 89% to *Cand*. Riegeria galateiae (FJ152947, EU440696, and GQ402753), all *Alphaproteobacteria* with completely sequenced genomes used in a previous phylogenomic study (16), and sequences for landmark genera of cultivated *Rhodospirillales*. Table S1 provides details on the *Cand*. Riegeria 16S rRNA sequences used, including accession numbers. Table S2 provides accession numbers of sequences from reference *Alphaproteobacteria* and the deltaproteobacterial outgroup. The sequences were

aligned by using MAFFT Q-INS-i, which considers the secondary structure of RNA (46), and the alignments were trimmed at the 5′ and 3′ ends. We evaluated the optimal substitution model of sequence evolution with MrModeltest (47), and the general time-reversible (GTR) model with invariable sites (I) and a γ-correction for site-to-site rate variation (G) model was selected using the Akaike information criterion. No filters based on sequence conservation were used. We reconstructed the phylogenies using neighbor joining-, parsimony- (both MEGA 4 software) (48), maximum likelihood- (PHYML; phylogeny.fr Web service) (49, 50), and Bayesian inference-based (MrBayes) (51) algorithms. MrBayes was run for 5 million generations and trees were sampled every 1,000 generations after a burn-in of 40%. Node stability was evaluated using bootstrap (1,000× neighbor joining and parsimony), pps (Bayesian inference), and aLRT [maximum likelihood (52, 53)]. Bootstrap support of at least 70%, aLRT of at least 80%, and posterior probabilities of at least 0.80 were considered statistically significant. Strict consensus trees were constructed by collapsing all nodes conflicting in different phylogenetic methods up to the lowest node supported by all methods.

18S and 28S rRNA gene datasets were constructed from *Paracatenula* host sequences and from selected Catenulida sequences available in GenBank, with sequences of rhabditophoran flatworms (Macrostomida) as outgroup. Accession numbers of all sequences are shown in Fig. S7 and Table S1. The 18S and 28S rRNA gene datasets were separately aligned and trimmed as for the 16S gene analysis. Substitution models were evaluated for each gene, and the GTR+I+G model was selected for both. We concatenated the alignments and then reconstructed and evaluated the phylogenies as described earlier for 16S rRNA genes.

Phylogenetic Analyses of DsrB, AprA, and CbbM. Analyses of all genes were based on amino acid translations by using MAFFT alignments of full-length reference sequences obtained from available genomes and partial, PCR-amplified fragments. The optimal Wehlan and Goldman substitution model (WAG) for the DsrB alignment (500 aa positions; WAG+G), the AprA alignment (376 aa positions; WAG+G+I), and the CbbM alignment (478 aa positions; WAG+G+I) was evaluated with MrModeltest. Phylogenies were reconstructed for all genes using PHYML as well as MrBayes (3 million generations, 1 million burn-in). Node support in all gene trees is indicated for the ML analysis by using PHYML (aLRT) and Bayesian inference (pp). aLRT of at least 80% and posterior probabilities of at least 0.80 were considered statistically significant.

FISH. We designed oligonucleotide FISH probes by using the arb probe design tool included in the arb software package (54) (Table S3) and evaluated their specificity in silico by using the probe match tool probeCheck (55). Fluorescently labeled probes were purchased from Thermo, and FISH was performed according to Manz et al. (56) as adapted for LR-white resin (British BioCell International) sections described in Nussbaumer et al. (57). As a negative control, a nonsense probe (NON-338) was used. To determine stringent hybridization conditions for the PAR1151 probe, a formamide series was conducted by using *Cand*. Riegeria galateiae cell extractions. All FISH experiments were examined by using a Leica TCS-NT confocal laser-scanning microscope.

ACKNOWLEDGMENTS. We thank the Core facility for Cell Imaging and Ultrastructural Research at the University of Vienna and M. Stachowitsch. This work was supported by Austrian Science Fund Projects P17710 (to S.B. and N.R.H.), P20185 (to A.L.), P20394 (to H.R.G.-V., U.D., and J.O.), P20775 (to K.S.), and Y277-B03 (to M.H.) and is contribution 902 from the Carrie Bow Cay Laboratory, Caribbean Coral Reef Ecosystem Program, National Museum of Natural History, Washington, DC. Part of this work was carried out with the use of the resources of the Computational Biology Service Unit of Cornell University, which is partially funded by Microsoft Corporation.

1. Sterrer W, Rieger RM (1974) Retronectidae - a new cosmopolitan marine family of Catenulida (Turbellaria). *Biology of the Turbellaria*, eds Riser N, Morse M (McGraw-Hill, New York), pp 63–92.
2. Ott JA, Rieger G, Rieger R, Enderes F (1982) New mouthless interstitial worms from the sulfide system: Symbiosis with Prokaryotes. *Pubblicazioni Stazione Zoologica Napoli I. Mar Ecol (Berl)* 3:313–333.
3. Dirks U, Gruber-Vodicka HR, Leisch N, Sterrer WE, Ott JA (2011) A new species of symbiotic flatworms, *Paracatenula galateia* n. sp. (Platyhelminthes: Catenulida: Retronectidae) from Belize (Central America). *Mar Biol Res*, 10.1080/17451000.2011.574880.
4. Ott JA, et al. (1991) Tackling the sulfide gradient: A novel strategy involving marine nematodes and chemoautotrophic ectosymbionts. *Pubblicazioni Stazione Zoologica Napoli I. Mar Ecol (Berl)* 12:261–279.
5. Giere O, Conway N, Gastrock G, Schmidt C (1991) "Regulation" of gutless annelid ecology by endosymbiotic bacteria. *Mar Ecol Prog Ser* 68:287–299.
6. Muller F, Brissac T, Le Bris N, Felbeck H, Gros O (2010) First description of giant *Archaea* (*Thaumarchaeota*) associated with putative bacterial ectosymbionts in a sulfidic marine habitat. *Environ Microbiol* 12:2371–2383.
7. Dubilier N, Bergin C, Lott C (2008) Symbiotic diversity in marine animals: The art of harnessing chemosynthesis. *Nat Rev Microbiol* 6:725–740.
8. Bright M, Sorgo A (2003) Ultrastructural reinvestigation of the trophosome in adults of *Riftia pachyptila* (Annelida, Siboglinidae). *Invertebr Biol* 122:347–368.
9. Pasteris JD, Freeman JJ, Goffredi SK, Buck KR (2001) Raman spectroscopic and laser scanning confocal microscopic analysis of sulfur in living sulfur-precipitating marine bacteria. *Chem Geol* 180:3–18.
10. Loy A, et al. (2009) Reverse dissimilatory sulfite reductase as phylogenetic marker for a subgroup of sulfur-oxidizing prokaryotes. *Environ Microbiol* 11:289–299.
11. Meyer B, Kuever J (2007) Molecular analysis of the diversity of sulfate-reducing and sulfur-oxidizing prokaryotes in the environment, using *aprA* as functional marker gene. *Appl Environ Microbiol* 73:7664–7679.
12. Badger MR, Bek EJ (2008) Multiple Rubisco forms in proteobacteria: Their functional significance in relation to CO_2 acquisition by the CBB cycle. *J Exp Bot* 59:1525–1541.
13. Stackebrandt E, Ebers J (2006) Taxonomic parameters revisited: Tarnished gold standards. *Microbiol Today* 33:152–155.
14. Wang Q, Garrity GM, Tiedje JM, Cole JR (2007) Naive Bayesian classifier for rapid assignment of rRNA sequences into the new bacterial taxonomy. *Appl Environ Microbiol* 73:5261–5267.
15. Williams KP, Sobral BW, Dickerman AW (2007) A robust species tree for the *Alphaproteobacteria*. *J Bacteriol* 189:4578–4586.
16. Wu D, et al. (2009) A phylogeny-driven genomic encyclopaedia of Bacteria and Archaea. *Nature* 462:1056–1060.
17. Murray RGE, Stackebrandt E (1995) Taxonomic note: implementation of the provisional status Candidatus for incompletely described procaryotes. *Int J Syst Bacteriol* 45:186–187.
18. Kanokratana P, et al. (2011) Insights into the phylogeny and metabolic potential of a primary tropical peat swamp forest microbial community by metagenomic analysis. *Microb Ecol* 61:518–528.
19. Loy A, et al. (2005) 16S rRNA gene-based oligonucleotide microarray for environmental monitoring of the betaproteobacterial order "Rhodocyclales". *Appl Environ Microbiol* 71:1373–1386.
20. Larsson K, Jondelius U (2008) Phylogeny of Catenulida and support for Platyhelminthes. *Org Divers Evol* 8:378–387.
21. Albuquerque L, Rainey FA, Nobre MF, da Costa MS (2008) *Elioraea tepidiphila* gen. nov., sp. nov., a slightly thermophilic member of the Alphaproteobacteria. *Int J Syst Evol Microbiol* 58:773–778.
22. Bright M, Bulgheresi S (2010) A complex journey: transmission of microbial symbionts. *Nat Rev Microbiol* 8:218–230.
23. Hurtado LA, Mateos M, Lutz RA, Vrijenhoek RC (2003) Coupling of bacterial endosymbiont and host mitochondrial genomes in the hydrothermal vent clam Calyptogena magnifica. *Appl Environ Microbiol* 69:2058–2064.
24. Stewart FJ, Young CR, Cavanaugh CM (2008) Lateral symbiont acquisition in a maternally transmitted chemosynthetic clam endosymbiosis. *Mol Biol Evol* 25:673–687.
25. Stewart FJ, Young CR, Cavanaugh CM (2009) Evidence for homologous recombination in intracellular chemosynthetic clam symbionts. *Mol Biol Evol* 26:1391–1404.
26. Moran NA, McCutcheon JP, Nakabachi A (2008) Genomics and evolution of heritable bacterial symbionts. *Annu Rev Genet* 42:165–190.
27. Moran NA, McLaughlin HJ, Sorek R (2009) The dynamics and time scale of ongoing genomic erosion in symbiotic bacteria. *Science* 323:379–382.
28. Ochman H, Elwyn S, Moran NA (1999) Calibrating bacterial evolution. *Proc Natl Acad Sci USA* 96:12638–12643.
29. Kuo CH, Ochman H (2009) Inferring clocks when lacking rocks: The variable rates of molecular evolution in bacteria. *Biol Direct* 4:35.
30. Douzery EJP, Snell EA, Bapteste E, Delsuc F, Philippe H (2004) The timing of eukaryotic evolution: does a relaxed molecular clock reconcile proteins and fossils? *Proc Natl Acad Sci USA* 101:15386–15391.
31. Distel DL (1998) Evolution of chemoautotrophic endosymbioses in bivalves. *Bioscience* 48:277–286.
32. Moran NA (1996) Accelerated evolution and Muller's rachet in endosymbiotic bacteria. *Proc Natl Acad Sci USA* 93:2873–2878.
33. Dale C, Wang B, Moran N, Ochman H (2003) Loss of DNA recombinational repair enzymes in the initial stages of genome degeneration. *Mol Biol Evol* 20:1188–1194.
34. Kuwahara H, et al. (2008) Reductive genome evolution in chemoautotrophic intracellular symbionts of deep-sea *Calyptogena* clams. *Extremophiles* 12:365–374.
35. Scott KM, et al. (2006) The genome of deep-sea vent chemolithoautotroph *Thiomicrospira crunogena* XCL-2. *PLoS Biol* 4:e383.
36. Sachs JL, Essenberg CJ, Turcotte MM (2011) New paradigms for the evolution of beneficial infections. *Trends Ecol Evol* 26:202–209.
37. Krieger J, Giere O, Dubilier N (2000) Localization of RubisCO and sulfur in endosymbiotic bacteria of the gutless marine oligochaete *Inanidrilus leukodermatus* (Annelida). *Marine Biology (Berlin)* 137:239–244.
38. Juretschko S, et al. (1998) Combined molecular and conventional analyses of nitrifying bacterium diversity in activated sludge: *Nitrosococcus mobilis* and *Nitrospira*-like bacteria as dominant populations. *Appl Environ Microbiol* 64:3042–3051.
39. Kane MD, Poulsen LK, Stahl DA (1993) Monitoring the enrichment and isolation of sulfate-reducing bacteria by using oligonucleotide hybridization probes designed

from environmentally derived 16S rRNA sequences. *Appl Environ Microbiol* 59: 682–686.
40. Pradillon F, Schmidt A, Peplies J, Dubilier N (2007) Species identification of marine invertebrate early stages by whole-larvae in situ hybridisation of 18S ribosomal RNA. *Mar Ecol Prog Ser* 333:103–116.
41. von Reumont BM, et al. (2009) Can comprehensive background knowledge be incorporated into substitution models to improve phylogenetic analyses? A case study on major arthropod relationships. *BMC Evol Biol* 9:119.
42. Meyer B, Kuever J (2007) Molecular analysis of the distribution and phylogeny of dissimilatory adenosine-5′-phosphosulfate reductase-encoding genes (*aprBA*) among sulfur-oxidizing prokaryotes. *Microbiology* 153:3478–3498.
43. Blazejak A, Kuever J, Erséus C, Amann R, Dubilier N (2006) Phylogeny of 16S rRNA, ribulose 1,5-bisphosphate carboxylase/oxygenase, and adenosine 5′-phosphosulfate reductase genes from gamma- and alphaproteobacterial symbionts in gutless marine worms (oligochaeta) from Bermuda and the Bahamas. *Appl Environ Microbiol* 72: 5527–5536.
44. Meyer H, et al. (2006) Soil carbon and nitrogen dynamics along a latitudinal transect in Western Siberia, Russia. *Biogeochemistry* 81:239–252.
45. Altschul SF, Gish W, Miller W, Myers EW, Lipman DJ (1990) Basic local alignment search tool. *J Mol Biol* 215:403–410.
46. Katoh K, Kuma K-i, Toh H, Miyata T (2005) MAFFT version 5: Improvement in accuracy of multiple sequence alignment. *Nucleic Acids Res* 33:511–518.
47. Nylander JAA (2008) *MrModeltest v2.3 Program Distributed by the Author* (Uppsala Univ, Uppsala, Sweden).
48. Tamura K, Dudley J, Nei M, Kumar S (2007) MEGA4: Molecular Evolutionary Genetics Analysis (MEGA) software version 4.0. *Mol Biol Evol* 24:1596–1599.
49. Guindon S, Gascuel O (2003) A simple, fast, and accurate algorithm to estimate large phylogenies by maximum likelihood. *Syst Biol* 52:696–704.
50. Dereeper A, et al. (2008) Phylogeny.fr: Robust phylogenetic analysis for the non-specialist. *Nucleic Acids Res* 36(suppl 2):W465–W469.
51. Ronquist F, Huelsenbeck JP (2003) MrBayes 3: Bayesian phylogenetic inference under mixed models. *Bioinformatics* 19:1572–1574.
52. Anisimova M, Gascuel O (2006) Approximate likelihood-ratio test for branches: A fast, accurate, and powerful alternative. *Syst Biol* 55:539–552.
53. Guindon S, et al. (2010) New algorithms and methods to estimate maximum-likelihood phylogenies: Assessing the performance of PhyML 3.0. *Syst Biol* 59:307–321.
54. Ludwig W, et al. (2004) ARB: A software environment for sequence data. *Nucleic Acids Res* 32:1363–1371.
55. Loy A, et al. (2008) probeCheck—a central resource for evaluating oligonucleotide probe coverage and specificity. *Environ Microbiol* 10:2894–2898.
56. Manz W, Amann R, Ludwig W, Wagner M, Schleifer K-H (1992) Phylogenetic oligodeoxynucleotide probes for the major subclasses of proteobacteria: Problems and solutions. *Syst Appl Microbiol* 15:593–600.
57. Nussbaumer AD, Fisher CR, Bright M (2006) Horizontal endosymbiont transmission in hydrothermal vent tubeworms. *Nature* 441:345–348.